



30th International Conference on Flexible Automation and Intelligent Manufacturing (FAIM2021)
15-18 June 2021, Athens, Greece.

New Approach for Beacons Based Mobile Robot Localization using Kalman Filters

A. Paulo Moreira^{a,b,*}, Paulo Costa^{a,b}, José Lima^{b,c}

^aFaculty of Engineering of University of Porto, Porto, Portugal

^bCentre for Robotics in Industry and Intelligent Systems - INESC TEC, Porto, Portugal

^cResearch Centre in Digitalization and Intelligent Robotics (CeDRI),

Instituto Politécnico de Bragança, Campus de Santa Apolónia,

5300-253 Bragança, Portugal

Abstract

New approaches on industrial mobile robots are changing the localization systems from old methods such as magnetic tapes to laser beacons based systems and natural landmarks since they are more adaptable and easier to install on the shop floor. Sensor fusion methods needs to be applied since there is information provided from different sources. Extended Kalman Filters are very used in the pose estimation of mobile robots with sensors that detect beacons and measure its distance and angle in a local referential frame. In certain situations, like for example wheels slippage, the number of impulses read for the encoders is wrong, resulting in a very large displacement or rotation and causing a bad estimation at the end of the prediction step. This bad estimation is used for the linearization of the non-linear equations, causing a bad linear approximation and probably a failure in the Kalman Filter. In this paper it is demonstrated that if we use the last state estimation calculated in the update step at the last cycle, instead of the estimation from the prediction step in the actual cycle, the result is an estimator much more robust to errors in the odometry information. Simulated and real results from several experiments are illustrated to demonstrate this new approach.

© 2020 The Authors. Published by Elsevier Ltd.

This is an open access article under the CC BY-NC-ND license (<https://creativecommons.org/licenses/by-nc-nd/4.0/>)

Peer-review under responsibility of the scientific committee of the FAIM 2021.

Keywords: Robot localization; Kalman Filter; Slippage

1. Introduction

Industrial mobile robots (Automatic Guided Vehicles, AGVs), are vehicles that can self-localize and move autonomously without human intervention. They are commonly used to transport materials between workstations in warehouses and production lines. They have been used in industrial environments for more than 50 years and both the algorithms and hardware, in which they rely on, have been evolving in order to increase the accuracy, robustness and flexibility, while decreasing the costs of construction and operation.

Actually, the Industry 4.0 concept requires that a mobile robot should decide and plan the trajectory to reach the goal

position, avoiding unknown obstacles and moving in a unstructured environment. The localization of the mobile robot is of crucial importance since it is needed to perform the correct path planning. Moreover, in industry environment, it is common to use beacons reflectors placed in specified places in order to the robots could localize themselves. It is also common to use a sensor fusion algorithm to combine several information provided by different sensors. One approach combined with the laser localization is the odometry that estimates the pose variation based on the wheels movement. In fact, this input allows to increase the localization accuracy but the slippage of the wheels deteriorates the localization estimation and can result in a fatal loss of the localization algorithm.

This paper proposes a new approach for mobile robots localization using an Extended Kalman Filter where, in certain random and timely situations, the estimated state obtained in the prediction phase is poor. Since in the correction phase, the linearization of the equations is calculated in the estimated state

* Corresponding author

E-mail addresses: amoreira@fe.up.pt (A. Paulo Moreira), paco@fe.up.pt (Paulo Costa), jllima@ipb.pt (José Lima).

resulting from the prediction phase, a wrong calculation of this linearization may lead to the filter diverging.

In a short cycle period and observations in every cycle, the state does not differ much from cycle to cycle. The innovative proposal of this approach is to linearize using the last estimate where there was a fusion with the observations as an alternative to linearize around the intermediate state obtained in the prediction phase.

A concrete example of this is the case of a mobile robot where odometry is generally relatively reliable, but in certain unforeseen situations one (or both) of the robot's wheels slide causing an estimate based on the equation of motion (prediction phase), very wrong. Even with a low slippage values, this occurrence may cause a divergence from the Kalman filter state estimate. This paper exemplifies this situation with a differential traction robot initially using simulations and then even using a real robot, showing its greater robustness without significantly affecting the estimate of the robot pose in normal situations. In order to test and validate the approach, a mobile robot, presented in figure 1 was developed. It is equipped with a YDLIDAR X4 lidar.

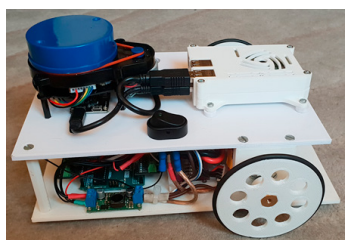


Fig. 1. Mobile robot.

The paper is organized as follows: after a brief introduction, section 2 presents the state of the art on the extended Kalman filtering procedures and the associated problems related to the non-linearities. Section 3 addresses the system architecture where the robot and simulation model are stressed. This section also presents the Ground-truth system that was used for validation. Section 4 proposes the algorithm to enhance the localization of a mobile robot based on odometry and beacons. Section 5 presents the results whereas last section rounds up the paper with conclusions and presents some future work.

2. Related work

For several years ago, a wide scientific community has been dedicated to the localization problem of mobile robots [12]. The extensive state of the art in this area proposes several solutions based on different algorithms with different types of sensors, starting from the oldest ones following a magnetic tape or line tracking [2, 3], to the modern lasers based on natural landmarks (Map Matching algorithm, as example), the reflector beacons [5, 10], image processing [7] or Wireless Sensor Network [8] such as Ultra wide band technology [11].

Odometry, brings unavoidable accumulated errors over long distances and needs to utilize the previous position to estimate

the next relative one and during which, the drift, the wheel slippage, the uneven floor and the uncertainty about the structure of the robot will together cause errors [9]. Due to this cumulative errors it is common to combine different localization methods.

Map matching algorithms are an important class of solutions based on the natural features of the environment [13]. However in industry, AGVs are commonly equipped with a laser scanner and the environment is populated by beacons (typically reflecting surfaces) [3].

The literature addresses the localization based on indistinguishable beacons, where the global localization is based on the observed distance between reflectors [6]. In this approach, odometry data from encoders sometimes is not used, and the global pose is computed without previous information on robot localization, while taking into account false detections (outliers). This approach results in a noisy estimation for the robot localization.

On the other hand, using an algorithm for sensorial data fusion in this problem is indeed relevant. It merges data from laser scanners (distances and angles measured from reflectors) with the odometry data.

In the specific case of localization estimation, sensors such as accelerometers, gyroscopes and encoders coupled to the wheels are typically used to estimate the robot movement from the last pose (dead reckoning). In the present paper, the odometry is used based on wheel encoders.

At the end, it is desired to estimate the robot state (position and orientation) from values of sensors that fits as much as possible with the observed data. From a mathematical perspective, there is a set of redundant observations, and the goal is to find the set of parameters that provides the best fit to the observed data that are corrupted by errors and the propagation of noise in the measurement process [1]. Moreover, robot environments are inherently unpredictable that combined to the measurement errors and noise can introduce wrong measurements [4].

There are some well-known algorithms capable of performing the sensor fusion, such as Bayesian networks, Maximum Likelihood and Maximum Posterior, Particle Filters and Kalman filter [1].

The extended Kalman filter can give reasonable performance and is the standard in navigation systems.

3. System Description

This section addresses the developed mobile robot to evaluate this approach. It is composed by a brief description of the robot, the simulation environment and the ground truth localization system used for real scenario.

3.1. Robot Hardware and mechanical description

A differential mobile robot prototype of 16 cm x 15 cm size and a distance between wells of 20 cm (figure 2) was developed having in mind the tests of the proposed methodology.

It is composed by two drive wheels and a castor wheel. Two DC motors drive the differential mobile robot, a typical config-

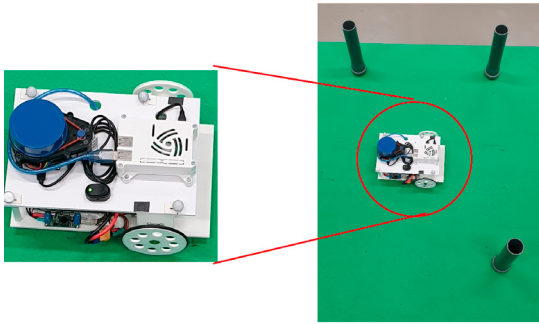


Fig. 2. Mobile robot and beacons layout.

uration in mobile robots. The maximum speed of the robot is 1 m/s but the tests presented in Results section were achieved with 10% of speed. It is powered by onboard 14.8 V LiPo battery and a DC/DC step down converter allows to supply the electronic modules composed by a Raspberry 3 model and arduino microcontroller board. The upper level is composed by a Raspberry microcomputer that runs raspbian operative system and is responsible for the Kalman filter processing, Wi-Fi communications and decision. The Arduino microcontroller boards deal with the low level control of motors, voltages, current, power management and odometry. It is equipped with a YDLIDAR X4 lidar that scans the 5 cm of diameter beacons (see figure 2 right).

3.2. Simulation Model

The simulation was implemented in the SimTwo environment. It is a realistic simulation system that can support several types of robots. Its main purpose is the simulation of mobile robots that can have wheels or legs, although industrial robots, conveyor belts and lighter-than-air vehicles can also be simulated. The dynamics realism in SimTwo is obtained by decomposing a robot in rigid bodies and electric motors. Each body behaviour is numerically simulated using its physical characteristics: shape, mass and moments of inertia, surface friction and elasticity. It is also possible to define standard joints such as socket, hinge and slider which can be coupled with an actuator or a sensor. More details about the SimTwo simulator can be found at [14]. Figure 3 presents the simulation environment where it can be seen three vertical beacons and the mobile robot. The time step of simulation control loop is 40 ms, the same as the real robot control.

3.3. Ground-Truth

Optical motion capture technology is a very useful tool for collecting and analysing positions and movements in several areas such as movement sciences, virtual reality, sports education, and robotics among the others [15]. Over the last decades, a variety of new systems have been developed [16].

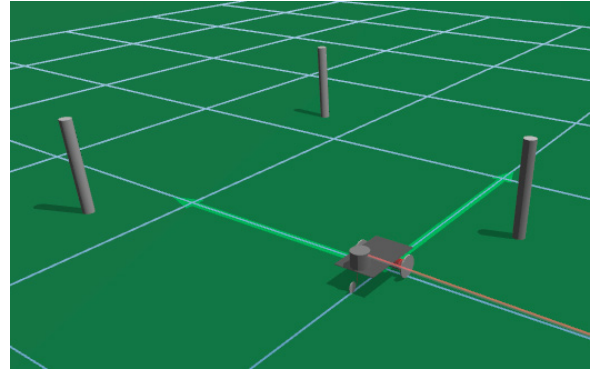


Fig. 3. Mobile robot and beacons layout on the simulation environment based on SimTwo.

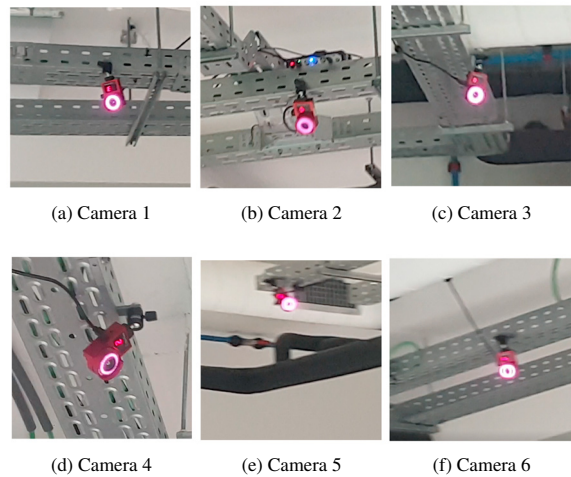


Fig. 4. Six OptiTrack cameras placed on the top

The ground truth system OptiTrack Motion Capture was used to compare the estimated positioning of our proposed system.

The OptiTrack, an isometric, passive marker-based optical motion capture system, consisted of six cameras in our case. The marker clusters used in this experiment were created using four spheres to triangulate the center point of the robot.

Figure 4 presents the six cameras placed on the top of the room.

4. Proposed Methodology

The model that is used is non-linear. So it is necessary to use an extended Kalman filter.

4.1. Extended Kalman Filter

The general motion model equation for an extended Kalman filter is presented in equation 1 where x_k is the state at time k ,

it has a non-linear relation, f , with the state at time $k - 1$, x_{k-1} , the input at time $k - 1$, u_{k-1} and the noise present at $k - 1$, w_{k-1} .

$$x_k = f(x_{k-1}, u_{k-1}, w_{k-1}) \quad (1)$$

In equation 2 the observation z_k at time k is also a non-linear function h of the state at time k and the noise v at time k .

$$z_k = h(x_k, v_k) \quad (2)$$

The equation 3 represents how the estimated observation \tilde{z}_k is calculated. This is also equation 2 where the noise is substituted by its mean value.

$$\tilde{z}_k = h(\tilde{x}_k, 0) \quad (3)$$

The equations 4, 5, 6 and 7 are the linearization of f and h with respect to the x , u , w and v .

$$A_{[i,j]} = \frac{\partial f_{[i]}}{\partial x_{[j]}}(\tilde{x}_{k-1}, u_k, 0) \quad (4)$$

$$H_{[i,j]} = \frac{\partial h_{[i]}}{\partial x_{[j]}}(\tilde{x}_k, 0) \quad (5)$$

$$W_{[i,j]} = \frac{\partial f_{[i]}}{\partial w_{[j]}}(\tilde{x}_{k-1}, u_k, 0) \quad (6)$$

$$V_{[i,j]} = \frac{\partial h_{[i]}}{\partial v_{[j]}}(\tilde{x}_k, 0) \quad (7)$$

In the equation 8, \tilde{x}_k^- is the state update from \tilde{x}_{k-1} . This results from equation 1 where the noise is substituted by its mean value.

$$\tilde{x}_k^- = f(\tilde{x}_{k-1}, u_{k-1}, 0) \quad (8)$$

The equation 9 presents the covariance state update, P_k^- where the Q_{k-1} is the covariance of w_{k-1} .

$$P_k^- = A_{k-1}P_{k-1}A_{k-1}^T + W_{k-1}Q_{k-1}W_{k-1}^T \quad (9)$$

Considering the R_{k-1} is the covariance of observation noise (v_{k-1}), equation 10 presents the estimated Kalman gain (K_k).

$$K_k = P_k^- H_k^T (H_k P_k^- H_k^T + V_{k-1} R_{k-1} V_{k-1}^T)^{-1} \quad (10)$$

In equation 11, \tilde{x}_k presents the updated state estimate, whereas equation 12 presents the updated covariance estimate, P_k With z_k equals to the measures provided by the sensors.

$$\tilde{x}_k = \tilde{x}_k^- + K_k(z_k - h(\tilde{x}_k^-, 0)) \quad (11)$$

$$P_k = (I - K_k H_k) P_k^- \quad (12)$$

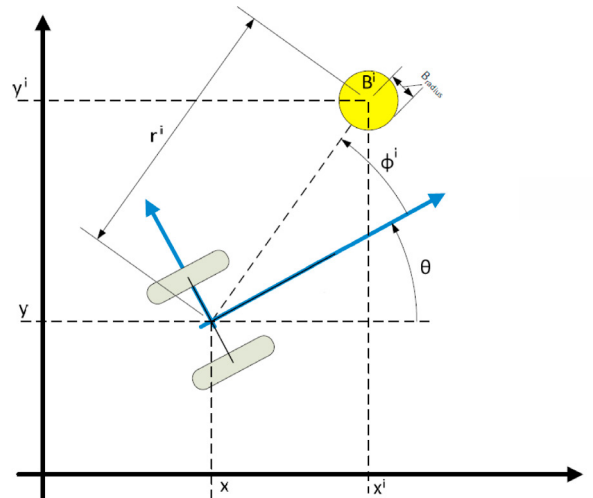


Fig. 5. Robot and reflector.

Assuming that the robot can detect up to L_{num} reflectors, equation 13 represents a set of pairs distance (r^i) and angle (θ^i) measured for each reflector. This setup is presented in figure 5.

$$\{Z_k^i = (r_k^i \ \phi_k^i)^T, c_k^i : i \in [1, L_{num}]\} \quad (13)$$

Equation 14 represent the robot pose (X_k) while in equation 15 u_k represent the input signals: Δd_k is the linear movement from the last sample and $\Delta \theta_k$ is the angular displacement from last sample. These values are estimated by the odometry system.

$$X_k = \begin{bmatrix} x_k \\ y_k \\ \theta_k \end{bmatrix} \quad (14)$$

$$u_k = \begin{bmatrix} \Delta d_k \\ \Delta \theta_k \end{bmatrix} \quad (15)$$

The equation 16 is the non-linear function used for the robot motion estimation.

$$f(X_k, u_k) = \begin{bmatrix} x_k + \Delta d_k \cos\left(\theta_k + \frac{\Delta \theta_k}{2}\right) \\ y_k + \Delta d_k \sin\left(\theta_k + \frac{\Delta \theta_k}{2}\right) \\ \theta_k + \Delta \theta_k \end{bmatrix} \quad (16)$$

From equation 4, the A_k matrix is presented in equation 17.

$$A_k = \begin{bmatrix} 1 & 0 & -\Delta d_k \sin\left(\theta_k + \frac{\Delta \theta_k}{2}\right) \\ 0 & 1 & \Delta d_k \cos\left(\theta_k + \frac{\Delta \theta_k}{2}\right) \\ 0 & 0 & 1 \end{bmatrix} \quad (17)$$

From equation 6, the W_k matrix is presented in equation 18.

$$W_k = \begin{bmatrix} \cos\left(\theta_k + \frac{\Delta \theta_k}{2}\right) & -\frac{1}{2} \Delta d_k \sin\left(\theta_k + \frac{\Delta \theta_k}{2}\right) \\ \sin\left(\theta_k + \frac{\Delta \theta_k}{2}\right) & \frac{1}{2} \Delta d_k \cos\left(\theta_k + \frac{\Delta \theta_k}{2}\right) \\ 0 & 1 \end{bmatrix} \quad (18)$$

Equation 19 represents the odometry covariance, Q_k .

$$Q_k = \begin{bmatrix} \sigma_{\Delta d}^2 & 0 \\ 0 & \sigma_{\Delta \theta}^2 \end{bmatrix} \quad (19)$$

Each pair of reflector measurement (distance r^i and angle θ^i) with additive noise, $N(0, R_k)$ of average 0 and covariance R_k is presented in equation 20 and equation 21.

$$\begin{bmatrix} r^i \\ \theta^i \end{bmatrix} = h(M^i, X_k) + N(0, R_k) \quad (20)$$

$$R_k = \begin{bmatrix} \sigma_r^2 & 0 \\ 0 & \sigma_\phi^2 \end{bmatrix} \quad (21)$$

Equation 22 presents the non-linear function for each reflector observation where $M^i = (x^i, y^i)$ are the coordinates of the reflector.

$$h(M^i, X_k) = \begin{bmatrix} \sqrt{(x^i - x_k)^2 + (y^i - y_k)^2} \\ \text{atan2}(y^i - y_k, x^i - x_k) - \theta_k \end{bmatrix} \quad (22)$$

From equation 5, the H_k matrix is presented in equation 23.

$$H_k = \begin{bmatrix} -\frac{x^i - x_k}{\sqrt{(x^i - x_k)^2 + (y^i - y_k)^2}} & -\frac{y^i - y_k}{\sqrt{(x^i - x_k)^2 + (y^i - y_k)^2}} & 0 \\ \frac{y^i - y_k}{\sqrt{(x^i - x_k)^2 + (y^i - y_k)^2}} & -\frac{x^i - x_k}{\sqrt{(x^i - x_k)^2 + (y^i - y_k)^2}} & -1 \end{bmatrix} \quad (23)$$

4.2. Innovative Extended Kalman Filter approach

When using an extended Kalman Filter, there are some cases where the estimated state obtained in the prediction phase is quite wrong. Once in the correction phase, the linearization of the equations is calculated in the estimated state from the prediction phase, it happens that there is a wrong calculation of this linearization which can take to the filter to diverge. With a very short cycle period and observations in almost every cycle, the state will not be not so different from cycle to cycle. The innovative approach is to perform the linearization using the last estimate when there was a fusion with the observations instead of making the linearization around the intermediate estimate obtained in the prediction phase.

A concrete example of this situation is the case of a mobile robot where the odometry is usually reliable, but in certain unpredictable cases, one (or both) robot wheels slides causing an estimate based on the equation of motion (prediction phase) wrong. Even with low slippage values, this occurrence can cause a divergence in the Kalman filter estimate. In this paper, this situation is exemplified with a differential traction robot using at the beginning simulations and after that a real robot, showing its greater robustness without significantly affecting the estimate of the robot’s pose in normal situations. The innovative approach will be stressed in slippage conditions and results will be presented in next section.

5. Results

In order to validate the proposed innovative Kalman filter adaptation, two experiments were done on simulation environment and three on the real mobile robot, as early presented. The presented section is splitted according to these experiments methods. Emphasizing the slippage on wheels, both experiments address the same tests without and with the proposed filter. On the conducted experiments, the state of the robot (x, y and θ) were acquired and the robot angle θ , where the advantage of the new approach is more clear, is presented. All the following graphics, green line presents the real angle of the robot (provided by simulator on simulation and provided by the Optitrack ground truth system on the real robot experiments) whereas the gray line presents the estimated angle as the output of the Kalman filter (sensor fusion).

5.1. Simulation Results

At the simulation environment, is was carried out three experiments. The first one was designed without any slippage and with the standard Kalman Filter. The beacons are placed on positions [x y]: [-0.27 0.4], [0.27 0.4] e [0.27 -0.4]. For the first simulation test, the robot starts at position [x y θ]=[-0.27 0 - $\pi/2$] and the target position is [0 0 0].

As it can be seen in figure 6, both lines are coincident that means the Kalman filter is computing correctly.

The second simulation experiment shows that when there is a slippage on a wheel, a standard Kalman filter approach will diverge (as presented in Figure 7).

Finally, yet on simulation environment, the proposed Kalman filter innovative approach shows that for the same conditions the Kalman filter results on a convergence.

By this way, it is promising the use of the proposed Kalman filter adaptation. Nevertheless, some similar experiments will be done with the real robot and will be addressed in next subsection.

5.2. Real Robot Results

The real robot was stressed with three different experiments, and each one without and with the proposed Kalman filter adaptation in order to validate it. First experiment apparatus was

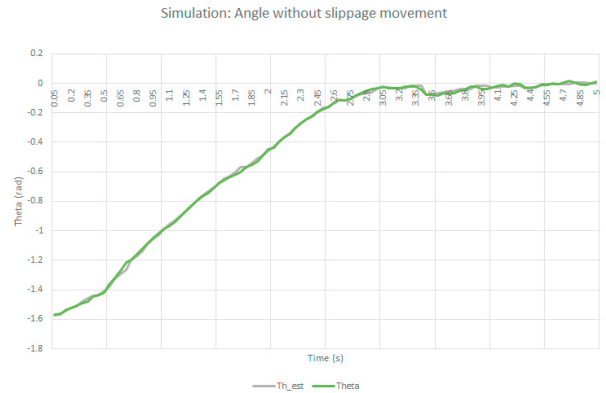


Fig. 6. Rotational movement with standard Kalman Filter estimation without slippage.

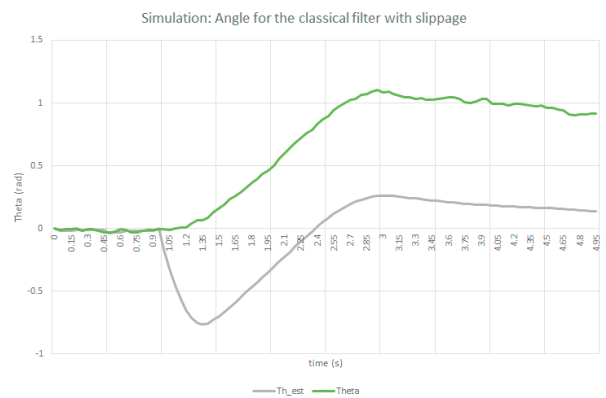


Fig. 7. Rotational movement with standard Kalman Filter estimation with slippage.

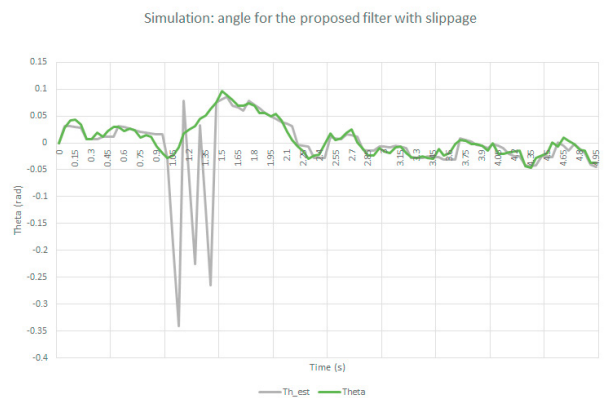


Fig. 8. Rotational movement with proposed Kalman Filter estimation with slippage.

based on keeping the robot still while suspended (this means the wheels rotate, like a trick to the filter). As stated in Figure 9,

the ground truth shows the root angle zero while the estimated angle is turning.

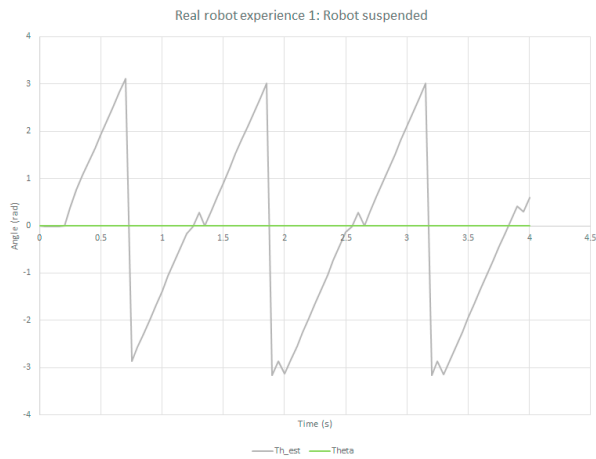


Fig. 9. Real robot suspended, without proposed filter.

The same experiment was conducted, but with the proposed Kalman Filter adaptation. This case is presented in Figure 10 that shows the Kalman filter is converging to the real state of the robot.

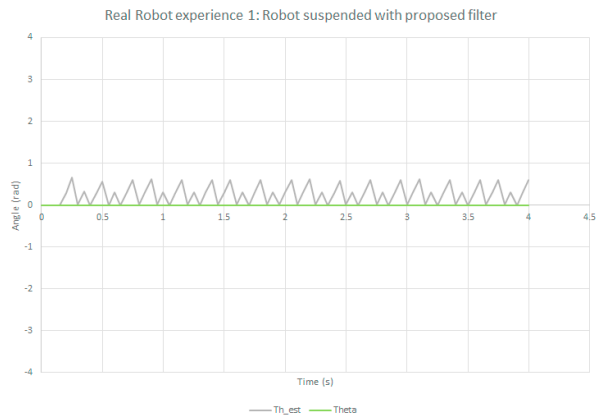


Fig. 10. Real robot suspended, with the proposed filter.

The second experiment condition is to make a linear movement to the robot. But in this case, one of the wheels will be removed the friction arc (that allow the wheel to hold the floor avoiding the slippage). In this case, presented in Figure 11, the output of the Kalman Filter will diverge.

When using the proposed approach, presented in Figure 12 it can be stated that the Kalman filter will converge to the real localization (presented the angle).

Last conducted experiment, experiment three, is presented on figure 13, where it is desired to turn the robot approximately one turn. In fact, without the proposed adaptation to the Kalman Filter, there will be an error of about 0.5 rads.

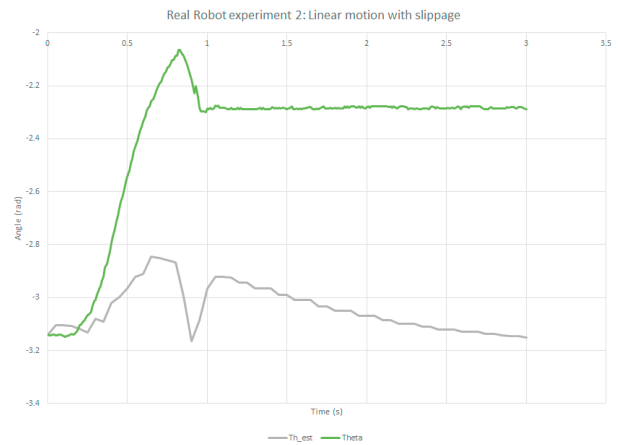


Fig. 11. Real experiment 2; Linear motion with slippage, without proposed filter.

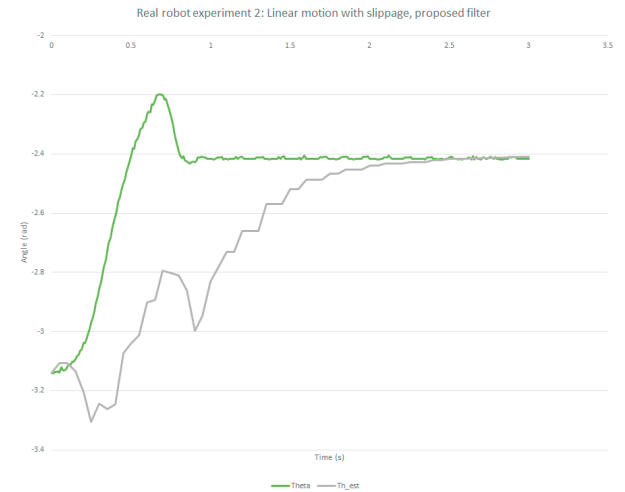


Fig. 12. Real experiment 2; Linear motion with slippage, with proposed filter.

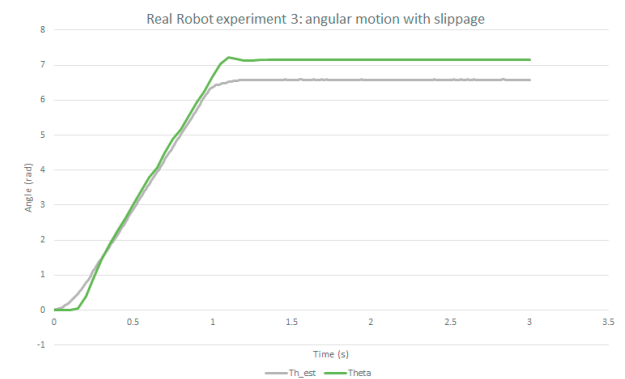


Fig. 13. Real experiment 3; Rotational motion with slippage, without proposed filter.

According to figure 14 where the innovative approach is introduced, the same experiment will tend the error to zero rads.

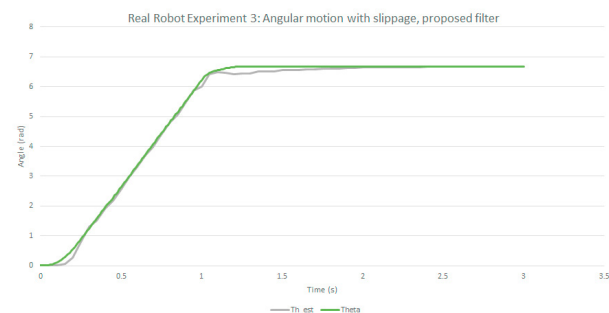


Fig. 14. Real experiment 3; Rotational motion with slippage, with proposed filter.

As a final remark, in all situations the proposed innovative Kalman filter adaptation will allow to converge the output even with strange input data (such as the slippage).

6. Conclusions and Future Work

This paper presented a new approach for mobile robot localization based on Extended Kalman Filter. The original Kalman Filter approach is well-known to observe, predict and fuse different data but in circumstances of slippage it will easily diverge, even with AGVs that typically have good odometry. The proposed solution was validated through simulation and using a real mobile robot, developed for this purpose. It was shown that the developed strategy is beneficial specially in the cases of slippage. The methodology that was addressed in this paper handles the error in odometry and thus can also be useful for different situations, such as floor with irregularities, ramps or wheels that are already worn out. At industry level this solution can be adopted in the presence of floors with debris or dirt.

As future work direction, it is pointed out the implementation and validation of the proposed approach for different robots types, such as tricycle and omnidirectional, among others.

Acknowledgements

This work is co-financed by the ERDF – European Regional Development Fund through the Operational Programme for Competitiveness and Internationalisation - COMPETE 2020 and the Lisboa2020 under the PORTUGAL 2020 Partnership Agreement, and through the Portuguese National Innovation Agency (ANI) as a part of project PRODUTECH SIF: POCI-01-0247-FEDER-024541.

This work is financed by the ERDF – European Regional Development Fund through the Operational Programme for Competitiveness and Internationalisation - COMPETE 2020 Programme, and by National Funds through the Portuguese funding agency, FCT - Fundação para a Ciência e a Tecnologia, within project SAICTPAC/0034/2015- POCI-01-0145-FEDER-016418.

References

- [1] Castanedo, F., "A Review of Data Fusion Techniques," *The Scientific World Journal*, vol. 2013, Article ID 704504, 19 pages, 2013. <https://doi.org/10.1155/2013/704504>.
- [2] L. Schulze and A. Wullner, "The Approach of Automated Guided Vehicle Systems," in *2006 IEEE International Conference on Service Operations and Logistics, and Informatics*, 2006, pp. 522-527.
- [3] L. Schulze, S. Behling, and S. Buhrs, "Automated Guided Vehicle Systems: a driver for increased business performance," in *Proceedings of the International MultiConference of Engineers and Computer Scientists*, 2008, pp. 19-21.
- [4] Thrun, S., Burgard, W., Fox, D., *Probabilistic Robotics (Intelligent Robotics and Autonomous Agents series)*, MIT series, 2005.
- [5] J. Borenstein, H. R. Everett, L. Feng and D. Wehe, "Mobile Robot Positioning and Sensors and Techniques", *Journal of Robotic Systems*, Special Issue on Mobile Robots, Vol. 14 No. 4, pp. 231-249, 1997.
- [6] Ronzoni, D., R. Olmi, C. Secchi, and C. Fantuzzi (2011). "AGV global localization using indistinguishable artificial landmarks". In: *IEEE International Conference on Robotics and Automation*, pp. 287–292.
- [7] D. Pizarro, M. Mazo, E. Santiso, M. Marron, D. Jimenez, S. Cobrecos and C. Losada, *Localization of Mobile Robots Using Odometry and an External Vision Sensor*, *Sensors* 2010, 10, pp. 3655-3680.
- [8] G. Fu, J. Zhang, W. Chen, F. Peng, P. Yang and C. Chen, *Precise Localization of Mobile Robots via Odometry and Wireless Sensor Network*, *International Journal of Advanced Robotic Systems*, 2013, Vol. 10, 203-213.
- [9] J. Borenstein and L. Feng, *Measurement and Correction of Systematic Odometry Errors in Mobile Robots*, *IEEE Transactions on Robotics and Automation*, Vol 12, No 6, pp. 869-880, 1996.
- [10] Lee, K., Lett Doh, N., Chung, W., Lee, S., Nam, S., *A robust localization algorithm in topological maps with dynamic noises*, *Industrial Robot*, Emerald, 2008.
- [11] Segura, M. J., Auat Cheein, F. A., Toibero, J. M., Mut, V., Carelli, R. (2011). *Ultra wide-band localization and SLAM: a comparative study for mobile robot navigation*. *Sensors (Basel, Switzerland)*, 11(2), 2035–2055. doi:10.3390/s110202035.
- [12] Pinto, Miguel; Moreira, Antonio Paulo; Matos, Anibal, *Localization of Mobile Robots Using an Extended Kalman Filter in a LEGO NXT*, *IEEE TRANSACTIONS ON EDUCATION*, Volume: 55 Issue: 1, Pages: 135-144 DOI: 10.1109/TE.2011.2155066, Published: FEB 2012 (ISI Web of Science Accession Number: WOS:000300058400017).
- [13] Heber Sobreira, A. Paulo Moreira, Paulo Costa José Lima, *Robust mobile robot localization based on a security laser: an industry case study*, *Industrial Robot: An International Journal*, Vol. 43 Iss 6 pp. 596 – 606 (<http://dx.doi.org/10.1108/IR-01-2016-0026>), 2016.
- [14] Costa, Paulo; Gonçalves, José; Lima, José; Malheiros, Paulo, *SimTwo realistic simulator: a tool for the development and validation of robot software*, *International Journal of Theory and Applications of Mathematics and Computer Science*. Str. Elena Drgoi, Romania. ISSN 2067-2764. p.17-33, 2011.
- [15] Webster, David and Celik, Ozkan, *Experimental evaluation of Microsoft Kinect's accuracy and capture rate for stroke rehabilitation applications*, *IEEE Haptics Symposium, HAPTICS*, doi 10.1109/HAPTICS.2014.6775498, ISBN 978-1-4799-3131-6, pp 455-460, 2014.
- [16] Clint Hansen , Jean-Louis Honeine , David Gibas , Nasser Rezzoug , Philippe Gorce and Brice Isableu, *Low-cost motion capture systems in practice*, *Computer Methods in Biomechanics and Biomedical Engineering*, 15:sup1, 253-255, DOI:10.1080/10255842.2012.713661, 2012.